

Additional Light Sterile Neutrinos and Cosmology

Thomas D. Jacques^{1,2}, Lawrence M. Krauss^{1,2}, and Cecilia Lunardini²

¹*School of Earth and Space Exploration, Arizona State University, Tempe AZ, 85287-1404 and*

²*Physics Department, Arizona State University, Tempe AZ, 85287-1404*

(Dated: January 14, 2013)

Tantalizing cosmological and terrestrial evidence suggests the number of light neutrinos may be greater than 3, motivating a careful re-examination of cosmological bounds on extra light species. Big Bang Nucleosynthesis constrains the number of relativistic neutrino species present during nucleosynthesis, $N_{\text{eff}}^{\text{BBN}}$, while measurements of the CMB angular power spectrum constrain the effective energy density in relativistic neutrinos at the time of matter-radiation equality, $N_{\text{eff}}^{\text{CMB}}$. There are a number of scenarios where new sterile neutrino species may have different contributions to $\Delta N_{\text{eff}}^{\text{BBN}}$ and $\Delta N_{\text{eff}}^{\text{CMB}}$, for masses that may be relevant to reconciling cosmological constraints with various terrestrial claims of neutrino oscillations. We consider a scenario with two sterile neutrinos and explore whether partial thermalization of the sterile states can ease the tension between cosmological constraints on $N_{\text{eff}}^{\text{BBN}}$ and terrestrial data. We then investigate the effect of a non-zero neutrino mass on their contribution to the radiation abundance, finding reductions in $\Delta N_{\text{eff}}^{\text{CMB}}$ of more than 5% for neutrinos with masses above 0.5 eV. While the effects we investigate here could play a role, we nevertheless find that two additional light sterile neutrinos species cannot fit all the data at the 95% confidence level.

I. INTRODUCTION

Neutrinos are unique among the known elementary particles in that their properties have often been first, and in general more, constrained by astrophysical and cosmological limits than by direct laboratory measurements. Already in the 1970s cosmological probes gave, first, a constraint on the neutrino mass based on estimates of the density of non-relativistic matter in the universe [1], and then a constraint on the number of light neutrino species based on estimates of primordial helium production during Big Bang Nucleosynthesis (BBN) [2–4]. Today, both of these probes have reached impressive sensitivity, and have started yielding some tantalizing suggestions of the possibility that extra neutrinos may be present in nature.

The radiation abundance in neutrinos and beyond-standard-model relativistic species is usually expressed as the effective number of relativistic species,

$$N_{\text{eff}} = \frac{\rho_{\text{rel}} - \rho_{\gamma}}{\rho_{\nu}^{\text{th}}}, \quad (1)$$

where $\rho_{\nu}^{\text{th}} = (7\pi^2/120)(4/11)^{4/3}T_{\gamma}^4$ is the energy density of one standard-model massless neutrino with a thermal distribution, ρ_{γ} is the energy density of photons and ρ_{rel} is total energy density in relativistic particles. In the standard model, by the time of BBN only the three known neutrino species contribute to ρ_{rel} , resulting in $N_{\text{eff}} = 3.046$ [5]. This is slightly larger than three due to reheating via e^+e^- annihilation.

Extra radiation beyond the standard model (the so called “dark” radiation), would cause an excess (which we label ΔN_{eff}) above the standard model value of N_{eff} . Although adding an extra light fermion could contribute $\Delta N_{\text{eff}} = 1$, most generally N_{eff} is non-integer

and varies with time, and depends on the physics at play. Specifically, lepton asymmetries [6, 7], particle decay [8, 9], partial thermalisation of new fermions [10, 11], the effect of a new MeV-scale particle on the active neutrino temperature [12], non-thermal production of dark matter [13] and heavy sterile neutrinos can all lead to contributions to N_{eff} that are not integer and/or change with time. Therefore we can hope that probing ΔN_{eff} precisely at different epochs – namely, during BBN and at the formation of the CMB – could discriminate between different models.

Recent measurements of N_{eff} have hinted at a value of $N_{\text{eff}} > 3.046$ ($\Delta N_{\text{eff}} > 0$). Constraints on N_{eff} can be derived from measurements of the primordial ^4He mass fraction, $Y_p \equiv \frac{4n_{\text{He4}}}{n_n + n_p}$, at BBN, $T \sim 0.2$ MeV. Izotov and Thuan [14] find $Y_p = 0.2565 \pm 0.0010(\text{stat.}) \pm 0.0050(\text{syst.})$, giving $N_{\text{eff}}^{\text{BBN}} = 3.68_{-0.70}^{+0.80}$ or $N_{\text{eff}}^{\text{BBN}} = 3.80_{-0.70}^{+0.80}$, each at 2σ , depending on the choice of the neutron lifetime, and assuming no lepton asymmetry. These are both more than 1σ from the standard model value. Other recent estimates of Y_p [15, 16] and various analyses of N_{eff} at BBN, e.g. [17–19], give for the most part central values more than 1σ above 3.

CMB constraints on N_{eff} are derived from measurements of the angular power spectrum at larger scales near the doppler peak, which can be used to constrain the redshift of matter-radiation equality ($T \sim 1$ eV). With independent measurements of the total matter abundance, this can also constrain the radiation abundance at matter-radiation equality. The South Pole Telescope suggests a somewhat high value, $N_{\text{eff}}^{\text{CMB}} = 3.71 \pm 0.35$ [20]. While evidence from WMAP 9 of an excess in N_{eff} is now reduced somewhat from earlier data sets [21], the actual value depends strongly

on which other observational data sets are combined with the WMAP data, with a new best-fit value of $N_{\text{eff}}^{\text{CMB}} = 3.26 \pm 0.35$ when all data sets are combined.

Interestingly, bounds from terrestrial searches for new physics on the masses and couplings of new particles invariably result in constraints on their contribution to the cosmological radiation, providing indirect constraints on ΔN_{eff} . Of particular interest are the recent hints of a fourth, sterile neutrino species from reactor neutrino experiments [22, 23], calibration data from Gallium-based solar neutrino detectors [24–26], and the Short Baseline (SBL) neutrino beam experiments LSND [27] and MiniBooNE [28–31] which search for $\bar{\nu}_\mu \rightarrow \bar{\nu}_e$ and $\nu_\mu \rightarrow \nu_e$ oscillations. All these generally support the existence of least one sterile neutrino with mass $\sim 0.1 - 1$ eV. This neutrino would be populated in the early universe via an interplay of oscillations and scattering, thus increasing N_{eff} .

Although the possibility of extra radiation due to sterile neutrinos seems to be substantiated at the general level, detailed analyses of the data reveal tensions between datasets and leave open the question of what scenario is most favored overall. MiniBooNE observes a difference between the muon neutrino and antineutrino disappearance rates, hinting at CP violating effects. The latest measurements by MiniBooNE show less tension between their neutrino/antineutrino results, although the $3+2$ scenario still provides a better fit to the data [31]. The simplest explanation for this is the existence of two sterile neutrinos families, although other data does not easily accommodate that possibility and the improvement in the global fit to the data may simply be due to the additional free parameters in a $3+2$ model [32–36]. Combined fits of SBL and cosmological data have found further tension when the sterile neutrinos are fully thermalized, with the level of tension depending on exactly which datasets are considered [37].

Whilst the cosmological data appear to rule out $N_{\text{eff}} = 5$, multiple sterile neutrinos can still be accommodated if one or more of them are not fully thermalized at the time of BBN. The degree of thermalization depends on the sterile neutrino mass and mixing parameters, as constrained by SBL data. Neutrino density evolution and partial thermalization in a $3+2$ scheme has been studied by Melchiorri et al. [11], finding tension both between the various terrestrial data sets, and between terrestrial and cosmological data. Since then, there have been substantial improvements in cosmological measurements and experimental results.

Considering that there is evidence from multiple sources that perhaps additional light neutrinos exist, and scenarios with two sterile neutrinos have been proposed as a way to explain the MiniBooNE results, it is important to re-examine cosmological constraints with

a more careful eye. With this goal in mind we have explored both partial thermalization of the sterile species at BBN and the effects that small neutrino masses will have on the relativistic neutrino fraction at the time of matter-radiation equality. As we will show, N_{eff} at BBN and CMB can be quite different for light neutrinos, but even incorporating this fact, and pushing all constraints to their 2σ level, cosmology can still not accommodate models with two such neutrinos.

II. PARTIAL THERMALIZATION IN A $3+2$ SCENARIO AND BBN CONSTRAINTS

We consider a scenario with two sterile neutrinos, and study the sensitivity of their thermalization efficiency to their masses and mixings. Specifically, we denote the two sterile neutrino flavors as ν_s and ν_r , and the corresponding mass eigenstates as m_4, m_5 , such that the mixing matrix U has entries $U_{s4} \simeq U_{r5} \simeq 1$, and the hierarchy $m_5 > m_4 \gg m_j$ ($j = 1, 2, 3$) holds. For simplicity, we also assume $U_{\tau 4} = U_{\tau 5} = 0$, so that our results for $N_{\text{eff}}^{\text{BBN}}$ only depend on $U_{e4}, U_{\mu 4}, U_{e5}, U_{\mu 5}$. We have verified that the complex phase $\eta = \text{Arg}(U_{e4}^* U_{\mu 4} U_{e5} U_{\mu 5}^*)$ does not affect the degree of thermalization, therefore we simplify the notation by considering U to be real.

In the density matrix formalism the differential equations governing evolution of the neutrino density are

$$\dot{\rho} = \mathcal{H}\rho - \rho\mathcal{H}^\dagger = i[H_m + V_{\text{eff}}, \rho] - \left\{ \frac{\Gamma}{2}, (\rho - \rho_{eq}) \right\}, \quad (2)$$

where ρ is the 5×5 neutrino density matrix in the flavor basis with diagonal entries corresponding to physical densities, \mathcal{H} is the full Hamiltonian, $H_m = U H_0 U^\dagger$ is a rotation of the free neutrino Hamiltonian in the mass basis $H_0 = \text{diag}(E_1, E_2, E_3, E_4, E_5)$, and ρ_{eq} is the density matrix at thermal equilibrium, $\rho_{eq} = I / (1 + e^{E/T})$. Equation (2) can be expressed as

$$\left(\frac{\partial \rho}{\partial T} \right)_{\frac{E}{T}} = -\frac{1}{HT} \left(i[H_m + V_{\text{eff}}, \rho] - \left\{ \frac{\Gamma}{2}, (\rho - \rho_{eq}) \right\} \right), \quad (3)$$

using the approximation $\dot{T} \simeq HT$, where $H = \sqrt{\frac{4\pi^3 g^*}{45}} \frac{T^2}{M_{\text{Pl}}}$ is the Hubble parameter, M_{Pl} is the Planck mass and g^* is the effective number of relativistic degrees of freedom. Since the full Hamiltonian is complex, the equation decomposes into a coherent commutator, and an anticommutator which describes loss of coherence. $V_{\text{eff}} = I(V_e, V_\mu, V_\tau, 0, 0)$ describes the effects of matter on the coherent part of the neutrino evolution. For zero lepton asymmetry,

$$V_\alpha = -A_\alpha \frac{2\sqrt{2}\zeta(3)}{\pi^2} \frac{G_F T^4 p}{m_W^2}, \quad (4)$$

where $A_e = 17$ and $A_{\mu,\tau} = 4.9$. $\Gamma = I(\Gamma_e, \Gamma_\mu, \Gamma_\tau, 0, 0)$ encodes decoherence and damping due to collisions with the background medium,

$$\Gamma_\alpha \simeq y_\alpha \frac{180\zeta(3)}{7\pi^4} G_F^2 T^4 p, \quad (5)$$

with $y_e = 3.6$, $y_{\mu,\tau} = 2.5$.

Before discussing the full numerical solution of Eqn. (3), we start with an approximate analytical solution for guidance in understanding the physics. Briefly (see Appendix for more details), the problem can be approximately reduced to two independent equations, each describing the population of one of the sterile species. For each sterile neutrino, (we use ν_s as an example in the following expressions) one can approximately use two independent oscillation channels, $\nu_e \rightarrow \nu_s$ and $\nu_\mu \rightarrow \nu_s$. For each channel, the effective mixing angle in vacuum is given by

$$\sin^2 2\theta_{\alpha s} \simeq 4U_{\alpha 4}^2 U_{s4}^2 \simeq 4U_{\alpha 4}^2, \quad \alpha = e, \mu, \quad (6)$$

while in-medium the mixing is suppressed according to the expression

$$\sin^2 2\theta_m \simeq \frac{\sin^2 2\theta_{\alpha s}}{(1 - b_\alpha(p, T))^2}, \quad (7)$$

$$b_\alpha(p, T) = \frac{2E V_\alpha}{\Delta m^2}. \quad (8)$$

One can then solve the evolution equation for f_s , the phase space distribution of ν_s , in terms of the interplay of oscillations and collisions. If f_s/f_α is energy-independent (i.e., a constant), and the mixing θ_m is well in the vacuum limit at the freezeout epoch, we find the contribution of ν_s to $N_{\text{eff}}^{\text{BBN}}$ to be

$$\Delta N_{\text{eff},s}^{\text{BBN}} = \frac{f_s}{f_\alpha} \simeq 1 - \exp \left[\frac{-2.06 \times 10^3}{\sqrt{g^*}} \left(\frac{m_4}{eV} \right) (U_{e4}^2 + 1.29U_{\mu 4}^2) \right]. \quad (9)$$

A similar expression holds for ν_r , with the substitutions $U_{\alpha 4}^2 \rightarrow U_{\alpha 5}^2$ and $m_4 \rightarrow m_5$. Ultimately, the total contribution of the two sterile states to N_{eff} is given by

$$\Delta N_{\text{eff}}^{\text{BBN}} \simeq \Delta N_{\text{eff},s}^{\text{BBN}} + \Delta N_{\text{eff},r}^{\text{BBN}}. \quad (10)$$

As expected, a sterile species is more populated at the time of BBN if oscillations are more efficient, i.e. for larger mixing (larger oscillation amplitude) and larger mass squared splitting relative to the active species, which means smaller oscillation length and therefore a higher probability of flavor conversion between two successive collisions. We also stress (see Appendix), that $\Delta N_{\text{eff},s}^{\text{BBN}}$ is larger for a larger collision rate; indeed, collisions favor the growth of the sterile population toward equilibrium [38] and in the

limit of no collisions (oscillations only), we would have $\frac{f_s}{f_\alpha} \leq (\sin^2 2\theta_{es} + \sin^2 2\theta_{\mu s})/2$, where the right hand side is the sum of the average vacuum oscillation probabilities in the two channels. Note that the production of ν_s, ν_r via oscillation from ν_μ is more efficient, because for the $\nu_\mu - \nu_s$ system the mixing angle is less suppressed by the thermal potential ($|V_\mu| < |V_e|$).

Let us now discuss the numerical solution. We follow the technique from Melchiorri et al. [11], numerically evolving the neutrino densities from temperatures of 100 MeV down to 1 MeV. To simplify the resultant set of differential equations, we assume a monochromatic neutrino energy distribution, with $E_\nu \simeq 3.15T$, rather than use the full spectrum of the neutrinos. This simplification has little effect on the density evolution [11].

We begin by running a loose scan across the allowed parameter space with the goal of finding reference points that minimize N_{eff} whilst also keeping m_4 and m_5 as low as possible, due to strong cosmological constraints on the sum of the neutrino masses. Constraints on the masses and mixing parameters are from SBL data [34]. As shown in Eqn. (9), the contribution of each sterile neutrino to N_{eff} is smallest when the two mixing matrix elements for that neutrino are minimized. However, SBL constraints on the product of the four mixing matrix elements prevent all four elements from being small. By definition, $m_5 > m_4$, and so it can be seen from Eqn. (9) that ν_r will have a larger contribution to $N_{\text{eff}}^{\text{BBN}}$ than ν_s for comparable mixing angles. For this reason, we focus on minimizing the thermalization of ν_s . Point 1 in Table I is chosen to correspond to the minimum values of $U_{e4}, U_{\mu 4}$ still allowed within 2σ . $U_{e5}, U_{\mu 5}$ are chosen to be as small as possible while satisfying constraints on $4|U_{e4} U_{\mu 4} U_{e5} U_{\mu 5}|$. m_4, m_5 are chosen to be as low as possible while still allowed by our choices of U_{ij} . This point does indeed lead to incomplete thermalization of ν_s , with $\Delta N_{\text{eff}}^{\text{BBN}} = 1.86$, as shown in Figure 1, although this is still outside the 2σ allowed range from Izotov and Thuan [14], $N_{\text{eff}}^{\text{BBN}} = 3.80^{+0.8}_{-0.7}$. In this region, the degree of thermalization is quite sensitive to $U_{e4}, U_{\mu 4}$. As an illustration, Figure 1 also shows the density evolution for two additional points in parameter space, labelled Points 2 and 3 in Table I, where $U_{e4}, U_{\mu 4}$ are pushed to even lower values, outside of the 2σ allowed region, but still within the 99 % C.L. allowed region. m_4, m_5 are kept fixed, and $U_{e5}, U_{\mu 5}$ are chosen to keep $4|U_{e4} U_{\mu 4} U_{e5} U_{\mu 5}|$ as close to the 2σ allowed region as possible while still remaining within the 2σ allowed region themselves. At Points 2 and 3, $\Delta N_{\text{eff}}^{\text{BBN}}$ is safely within the Izotov and Thuan 2σ allowed range.

	U_{e4}	$U_{\mu 4}$	U_{e5}	$U_{\mu 5}$	m_4 (eV)	m_5 (eV)	ΔN_{eff} (BBN)	ΔN_{eff} (z_{eq})	$\sum m_{\nu_s}^{\text{eff}}$ (eV)
Pt.1	0.055	0.034	0.13	0.13	0.6	0.9	1.86	1.68	1.31
Pt.2	0.040	0.025	0.17	0.17	0.6	0.9	1.63	1.47	1.18
Pt.3	0.030	0.016	0.17	0.17	0.6	0.9	1.40	1.25	1.14

TABLE I. Mass, mixing parameters, results for ΔN_{eff} at BBN and z_{eq} , and effective mass sum for the three sample points discussed in the text. The derivation of the final three columns is discussed in Sections II and III.

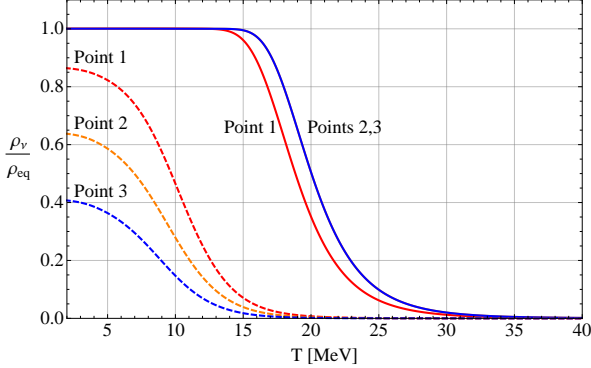


FIG. 1. Sterile neutrino density evolution as a fraction of the thermal density ρ_{eq} , for the masses and mixing angles listed in Table I. Dashed lines are for ν_s , solid lines are for ν_r .

III. PARTIAL THERMALIZATION AND PARTIALLY RELATIVISTIC NEUTRINOS IN A $3+2$ SCENARIO: CMB CONSTRAINTS

Both the position of the lowest peaks in CMB angular power spectrum and the damping tail at high multipole moments, l , are sensitive to the redshift at matter-radiation equality, and hence to the energy density of relativistic neutrinos at that time. The latter is usually expressed as a constraint on the sum of the neutrino masses,

$$\sum m_\nu = 94 \text{eV} (\Omega_{\nu, m} h^2), \quad (11)$$

where Ω is the density as a fraction of the critical density of the Universe, $\Omega = \rho/\rho_c$, and $\Omega_{\nu, m}$ is the neutrino contribution to the matter abundance Ω_m . It is important to note that in Eqn. (11) it is assumed that each species is fully thermalized, by assuming that for each species, $\rho_\nu^{\text{non-rel}} = m_\nu n_\nu^{\text{th}}$, with n_ν^{th} from Eqn. (14). Constraints on the sterile neutrino mass are really constraints on the product $m_\nu n_\nu$, and if a sterile neutrino does not undergo full thermalization, then it contributes $m_{\text{eff}} = m_\nu \frac{n_\nu}{n_\nu^{\text{th}}}$ to constraints on $\sum m_\nu$. For the partially thermalized $m_\nu = 0.6$ eV neutrino we consider in Table I, the phase space distribution is approximately a scaled Fermi-Dirac distribution as

shown in the Appendix, and $\frac{n_\nu}{n_\nu^{\text{th}}} = \Delta N_{\text{eff}}^{\text{CMB}}$. In Table I we show the effective $\sum m_\nu$ for the three points we consider.

In addition, many upper limits on the sum of the neutrino masses assume the standard model value of N_{eff} , and so do not directly apply to sterile neutrinos; However, a number of groups have constrained the $N_{\text{eff}} - \sum m_\nu$ plane using various combinations of measurements of the CMB, Hubble constant, baryon acoustic oscillations, and galaxy clusters [39–42]. For the value of N_{eff} we are interested in, detailed below, $\sum m_\nu \gtrsim 0.7$ eV is excluded at the 95% confidence level, which is inconsistent with the values shown in Table I for all 3 points. (Tension between SBL and cosmological data is also discussed in Ref. [43] in the context of two fully thermalized neutrinos.)

There is another, equally important factor that can affect the value of N_{eff} that should be utilized when applying cosmological constraints: the fact that neutrinos may not be fully relativistic at the time of matter-radiation equality.

The standard model neutrino temperature at matter-radiation equality is $T_\nu = 0.55$ eV [21]. [44]. N_{eff} as derived from the CMB measures the relativistic energy density at the time of matter-radiation equality. A neutrino with $m_\nu \sim \mathcal{O}(1\text{eV})$ will not be entirely relativistic at this time, and so will contribute $\Delta N_{\text{eff}} \lesssim 1$. Constraints on N_{eff} are continually getting tighter, and so this can be an important effect for sterile neutrinos towards the top of the allowed mass range. A similar effect was considered in Ref. [45], where the scale factor at matter-radiation equality was related to the mass and energy density of a sterile neutrino.

The pressure density provides a convenient measure of how relativistic a particle is at any given temperature, with $P = \rho/3$ for fully relativistic particles and $P = 0$ for non-relativistic particles. As the sterile neutrinos become less relativistic, their pressure drops below $\rho/3$, and the relativistic fraction of their energy density drops accordingly,

$$\rho_\nu^{\text{rel}} = \rho_\nu \left(\frac{P_\nu}{\rho_\nu} \right) \left(\frac{1}{3} \right), \quad (12)$$

using $P_\nu^{\text{th}}/\rho_\nu^{\text{th}} = 1/3$ when $m = 0$. With this, the effective number of relativistic degrees of freedom can be expressed as

$$N_{\text{eff}} = \frac{\rho_\nu^{\text{rel}}}{\rho_{\nu, m=0}^{\text{th}}} = \frac{P_\nu}{P_{\nu, m=0}^{\text{th}}}. \quad (13)$$

The number, pressure and energy densities are given

by the standard formulae,

$$n_\nu = \frac{g}{2\pi^2} \int dp p^2 f_\nu(p), \quad (14)$$

$$P_\nu = \frac{g}{2\pi^2} \int dp \frac{p^4}{3E} f_\nu(p), \quad (15)$$

$$\rho_\nu = \frac{g}{2\pi^2} \int dp E p^2 f_\nu(p), \quad (16)$$

where g counts the number of helicity states, $f_\nu(p)$ is the neutrino phase-space distribution, and $p = |\vec{p}|$. When the neutrinos are in thermal equilibrium, they

follow a Fermi-Dirac distribution,

$$f_\nu(p) = \frac{1}{1 + \exp[\frac{E}{T}]}, \quad (17)$$

when the chemical potential is zero. After freezeout at $T_F \sim 2$ MeV, the co-moving number density must be conserved:

$$\begin{aligned} n_\nu(p, T) &= \left(\frac{a_F}{a}\right)^3 n_\nu(p_F, T_F) \\ &= \left(\frac{a_F}{a}\right)^3 \frac{g}{2\pi^2} \int dp_F p_F^2 \frac{1}{1 + \exp[\frac{E_F}{T_F}]}, \end{aligned} \quad (18)$$

where a is the scale factor, and subscript F denotes the value at freezeout. Neutrino momentum redshifts as $p = (\frac{a_F}{a}) p_F$, and so the neutrino number density after freezeout is

$$\begin{aligned} n_\nu(p, T) &= \left(\frac{a_F}{a}\right)^3 \frac{g}{2\pi^2} \int \left(\frac{a}{a_F} dp\right) \left(\frac{a}{a_F} p\right)^2 \frac{1}{1 + \exp[\frac{\sqrt{(\frac{a}{a_F} p)^2 + m^2}}{T_F}]} \\ &= \frac{g}{2\pi^2} \int dp p^2 \frac{1}{1 + \exp[\frac{\sqrt{(\frac{a}{a_F} p)^2 + m^2}}{T_F}]} \end{aligned} \quad (19)$$

Comparing this with Eqn. (14) and using $T = T_0/a$, we have

$$f_\nu(p) = \left(1 + \exp\left[\frac{\sqrt{\left(\frac{T_F p}{T}\right)^2 + m^2}}{T_F}\right]\right)^{-1} \quad (20)$$

after freezeout. This reduces to the standard expression for both relativistic and non-relativistic particles. N_{eff} can then be found using Eqn. (13) with Eqns. (15, 20). Since the co-moving number density is conserved from the time when the neutrinos were entirely relativistic, it follows that the number density dn/dp must be independent of mass. Thus the total neutrino energy density $d\rho/dp = \sqrt{p^2 + m^2} dn/dp$ will be larger for particles with larger mass. This is compensated for by the fact that the pressure is smaller for massive neutrinos, leading massive sterile neutrinos to have a smaller contribution to N_{eff} as shown in Figs. 2 and 3.

We use this relation to determine the relevant values of N_{eff} at matter-radiation equilibrium for the $3 + 2$ sterile neutrino models discussed earlier to explore whether they may be consistent with both SBL and cosmological bounds, and report the results in Table 1 [46]. The use of Eqn. (13) to determine N_{eff} requires knowledge of the neutrino phase-space distribution at decoupling, and we demonstrate in the appendix that our three points satisfy the conditions required for the phase-space distribution to be approximated by a Fermi-Dirac distribution scaled by a constant. With this approximation, and using Eqn. (13) with Eqns. (15, 20), the contribution to N_{eff} at z_{eq} are $\Delta N_{\text{eff}} = (1.68, 1.47, 1.25)$ at Points 1, 2, and 3 respectively. This leads to some easing of the tension between SBL data and CMB constraints on N_{eff} .

IV. DISCUSSION AND CONCLUSIONS

We have discussed the cosmological generation and evolution of a population of two sterile neutrinos, with masses and mixings motivated by the recent SBL data. Specifically, we calculated the contribution of these extra neutrino species to N_{eff} at BBN and CMB epochs. We focused on the region of the parameter space where the sterile neutrinos are produced with less than thermal abundance ($\Delta N_{\text{eff}} < 2$), so that the tension with BBN and CMB measurements is eased, compared with the case of two fully thermalized species. We find points at the limit of the region of parameter space allowed by the SBL data where the heaviest sterile state is fully thermalized, while the second is produced with

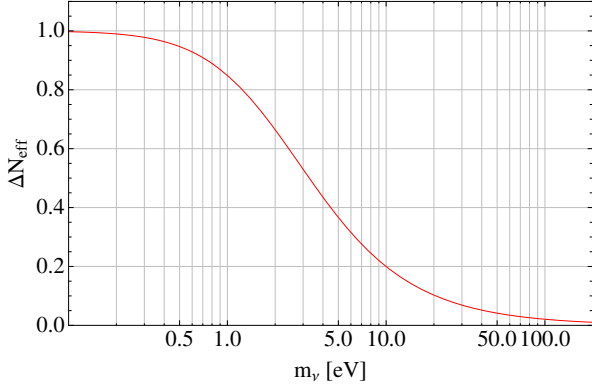


FIG. 2. Contribution of one thermalized massive sterile neutrino to N_{eff} at the time of matter-radiation equality. If the sterile neutrino has an approximately Fermi-Dirac distribution, this is equivalent to $\Delta N_{\text{eff}}^{z_{\text{eq}}} / \Delta N_{\text{eff}}^{\text{BBN}}$, i.e. if the sterile neutrino is not fully thermalized and $\Delta N_{\text{eff}}^{\text{BBN}} < 1$, then $\Delta N_{\text{eff}}^{z_{\text{eq}}}$ will be reduced accordingly.

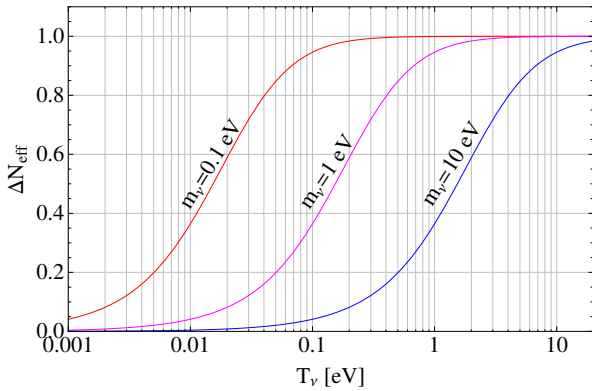


FIG. 3. Contribution of one massive sterile neutrino to N_{eff} as a function of the equivalent temperature of a massless neutrino, T_ν . At matter-radiation equality, $T_\nu = 0.55$ eV [21].

abundance as low as $\sim 40\%$ of the thermal abundance.

Whilst it is possible – with the maximum suppression of N_{eff} due to partial thermalization – to find points in parameter space marginally compatible with BBN constraints ($N_{\text{eff}}^{\text{BBN}} \lesssim 4.6$ at 2σ), the tension with BBN data overall remains.

Interestingly, if SBL-favored sterile neutrinos really are the origin of $N_{\text{eff}} > 3$, we expect their contribution to N_{eff} at z_{eq} – relevant for CMB constraints – to be lower than that at BBN epoch, due to their being only moderately (partially) relativistic at z_{eq} . In principle, this feature would allow us to distinguish the sterile neutrino hypothesis from other possible origins of an excess of radiation, however the difference $N_{\text{eff}}^{\text{BBN}} - N_{\text{eff}}^{\text{CMB}}$ is on the order of 10% or less. It is not

clear whether foreseeable probes of N_{eff} at different epochs will ever reach this level of precision. We also note that while the mass-induced suppression works to ease the tension with the CMB data somewhat, it comes with a price: the ~ 1 eV masses of the sterile states would increase the sum of the neutrino masses to $\sum m_\nu > 1$ eV, which is disfavored by CMB bounds on this quantity.

Summing up, we find that even with the suppression effects due to partial thermalization and partially relativistic masses, two additional sterile neutrinos in a mass range that might explain SBL neutrino data appear to be inconsistent with cosmological bounds coming from BBN and CMB measurements.

It has recently been questioned whether the SBL data from MiniBooNE actually favor 2 sterile neutrinos [31]. If this requirement is relaxed then the results we derive will be particularly relevant to constrain models with one extra neutrino. Alternatively, new physics that might resolve these inconsistencies include altering microphysics or altering cosmology. An example of the former includes introducing a lepton asymmetry in addition to the two sterile neutrinos [47–49]. For example, it has recently been shown that large lepton asymmetries do lead to incomplete thermalization in a scenario with one sterile neutrino [7]. As an example of the latter, Hamann et al. [19] find that models with one fully thermalized eV-scale sterile neutrino and additional massless degrees of freedom can provide a better fit to a wide range of cosmological data than standard Λ CDM, if the dark energy equation of state parameter is free to be $w < -1$. Nevertheless this requires a contribution to N_{eff} from massless sterile states of $\Delta N_{\text{eff}} > 1$, and is thus in tension with BBN constraints on Y_p , unless the standard model neutrinos have a non-zero chemical potential.

The need to consider such exotic possibilities to possibly obviate the bounds we derive here demonstrates, once again, the important utility of cosmological observations on constraining fundamental neutrino particle physics.

ACKNOWLEDGMENTS

LMK and TDJ acknowledges support from the DOE for this work; CL and TDJ acknowledge the support of the NSF under Grant No. PHY-0854827.

Appendix A: Analytical Approximation

Let us derive the approximate analytical result for $\Delta N_{\text{eff}}^{\text{BBN}}$, Eqs. (9)-(10).

1. Oscillation amplitude in vacuum and in medium

We consider a basis of 5 neutrino flavor states (ν_α , $\alpha = e, \mu, \tau, s, r$), where ν_s, ν_r are the sterile states. These are related to the mass eigenstates by the mixing matrix U , $\nu_\alpha = \sum_{i=1,5} U_{\alpha i} \nu_i$, where $U_{s4} \simeq U_{r5} \simeq 1$ and U is taken to be real for simplicity. As stated in the main text, we use a number of assumptions to simplify the problem: (i) $U_{s5} = U_{r4} = 0$ (ii) $U_{\tau 4} = U_{\tau 5} = 0$, (iii) mass hierarchy $m_5 > m_4 \gg m_j$.

Let us find the amplitude of active-sterile oscillations in vacuum, by calculating $P(\nu_\alpha \rightarrow \nu_s)$ (for definiteness; analogous results hold for ν_r), with $\alpha = e, \mu$. The channel $\nu_\tau \rightarrow \nu_s$ has zero probability due to assumption (ii). We use the standard notation $\Delta m_{ij}^2 = m_i^2 - m_j^2$.

In all generality, the standard oscillation formalism gives

$$P(\nu_\alpha \rightarrow \nu_s) = -4 \sum_{i,j,i>j} U_{\alpha i} U_{s i} U_{\alpha j} U_{s j} \sin^2 \left(\frac{\Delta m_{ij}^2}{4E} t \right). \quad (\text{A1})$$

Using assumption (i) and neglecting the lowest oscillation frequencies (assumption (iii)), we get:

$$\begin{aligned} P(\nu_\alpha \rightarrow \nu_s) &\simeq -4 U_{\alpha 4} U_{s 4} \sum_{i=1,2,3} U_{\alpha i} U_{s i} \sin^2(\omega_s t), \\ &\simeq 4 U_{\alpha 4}^2 U_{s 4}^2 \sin^2(\omega_s t), \end{aligned} \quad (\text{A2})$$

where $\omega_s = m_4^2/(4E)$, and the last expression is obtained using the unitarity of the mixing matrix. Eq. (A2) has the same form as the classic 2-neutrino oscillation probability, with effective mixing

$$\sin^2 2\theta_{\alpha s} \equiv 4 U_{\alpha 4}^2 U_{s 4}^2 \simeq 4 U_{\alpha 4}^2. \quad (\text{A3})$$

An analogous result is obtained for ν_r , with $\omega_r = m_5^2/(4E)$ and $\sin^2 2\theta_{\alpha r} \simeq 4 U_{\alpha 5}^2$. It is immediate to verify that, under the same assumptions as above, $P(\nu_\alpha \rightarrow \nu_r) = P(\nu_r \rightarrow \nu_\alpha)$ and $P(\nu_\alpha \rightarrow \nu_s) = P(\nu_s \rightarrow \nu_\alpha)$.

Due to the thermal refraction potential, the effective, two-neutrino oscillation amplitude is suppressed – for both neutrinos and antineutrinos – as follows (see, e.g., [50]):

$$\sin^2 2\theta_m \simeq \frac{\sin^2 2\theta_{\alpha s}}{(1 - b_\alpha(p, T))^2}, \quad (\text{A4})$$

$$b_\alpha(p, T) = \frac{2E V_\alpha}{\Delta m^2}, \quad (\text{A5})$$

where V_α is as in Eqn. (4) and we used $\cos 2\theta_{\alpha s} \simeq 1$, for convenience in the calculations that follow. The expression (A5) is valid for a CP-symmetric neutrino gas; the more complicated case with a lepton asymmetry will not be discussed here.

2. Flavor evolution equation and its solution

Let us now consider the production of the sterile neutrino ν_s , using an effective two-neutrino system, $\nu_\alpha - \nu_s$ with the oscillation frequency and amplitude as outlined above. Let f_s and f_α be the phase space distributions of ν_s and of one of the active species, and let p be the neutrino momentum. We start with the evolution equation (see e.g., Foot and Volkas [50] and Dodelson and Widrow [51]),

$$\begin{aligned} \left(\frac{\partial}{\partial t} - H E \frac{\partial}{\partial E} \right) f_s(E, t) = \\ \sin^2 2\theta_m(E, t) \frac{\Gamma_\alpha(E, t)}{4} (f_\alpha(E, t) - f_s(E, t)) \end{aligned} \quad (\text{A6})$$

with Γ_α being the collision rate, Eqn. (5). Eq. (A6) is valid when the neutrino oscillation length is much shorter than the neutrino mean free path, so that the effect of oscillations between two collisions is described by the averaged in-medium oscillation probability $\langle P \rangle = \sin^2 2\theta_m/2$. We have verified that this is always the case for our parameters of interest [52]. We take $f_\alpha = f_\alpha(p/T)$ to be a Fermi-Dirac distribution, but the derivation in this section holds for any function of p/T .

Eqn. (A6) can be simplified using [51]

$$\left(\frac{\partial}{\partial t} - H E \frac{\partial}{\partial E} \right) = -H T \frac{\partial}{\partial T} \Big|_y, \quad y \equiv p/T \quad (\text{A7})$$

and defining

$$\begin{aligned} x &\equiv \frac{2^{5/4}}{\pi M_W} \sqrt{A_\alpha \zeta(3)} G_F \frac{T^3}{m_4} \\ &\simeq 3.53 \times 10^{-5} \sqrt{A_\alpha} \left(\frac{T}{\text{MeV}} \right)^3 \left(\frac{\text{eV}}{m_4} \right) \end{aligned} \quad (\text{A8})$$

so that $-b_\alpha(p, T) \equiv y^2 x^2$. Thus, we have the new equation

$$-H T \frac{\partial f_s}{\partial T} = \frac{\sin^2 2\theta_{\alpha s} \Gamma_\alpha(y, x)}{2(1 + x^2 y^2)^2} (f_\alpha(y) - f_s(x, y)), \quad (\text{A9})$$

where y and x should be treated as independent variables, and the differential equation should be solved with respect to x , with y fixed.

Changing the differentiation variable from T to x [51], and neglecting the temperature dependence of g^* , one finds a solution of the form

$$\begin{aligned} 1 - \frac{f_s}{f_\alpha} &= \exp \left[-\frac{m_4}{m_f} U_{\alpha 4}^2 \frac{y_\alpha}{\sqrt{A_\alpha}} \int_{xy}^\infty \frac{d(x'y)}{(1 + (x'y)^2)^2} \right], \\ m_f &\simeq \frac{13\sqrt{g^*}}{G_F^{3/2} M_{\text{pl}} M_W} \simeq 1.05 \times 10^{-3} \text{ eV}, \end{aligned} \quad (\text{A10})$$

where $g^* = 10$ has been used. As discussed in Ref. [51], if the lower integration limit is small, i.e. $xy \ll 1$

($-b_\alpha(p, T) \ll 1$) at freezeout, we can replace it with 0, thus solving the integral exactly, with $\pi/4$ as the result. In this limit, f_s/f_α is independent of y [51], meaning that f_s has the same spectral shape as f_α , and the two only differ by an overall factor. For the freezeout temperature $T_\nu \simeq 2$ MeV, and for $p = 3.15T$, we get $xy \simeq 4 \times 10^{-3} m_4/\text{eV}$, so this condition holds for the range of masses of interest here.

The final result for the ratio f_s/f_α is then

$$\frac{f_s}{f_\alpha} = 1 - \exp \left[-\frac{\pi}{4} \frac{m_4}{m_f} U_{\alpha 4}^2 \frac{y_\alpha}{\sqrt{A_\alpha}} \right]. \quad (\text{A11})$$

In the limit $f_s/f_\alpha \ll 1$, an expansion of the exponential recovers the result in [11, 51].

For our case, where two oscillation channels are present, $\nu_s \leftrightarrow \nu_e$ and $\nu_s \leftrightarrow \nu_\mu$, the generalization is

immediate:

$$\begin{aligned} \frac{f_s}{f_\alpha} &= 1 - \exp \left[-\frac{\pi}{4} \frac{m_4}{m_f} \left(U_{e4}^2 \frac{y_e}{\sqrt{A_e}} + U_{\mu 4}^2 \frac{y_\mu}{\sqrt{A_\mu}} \right) \right] \\ &\simeq 1 - \exp \left[\frac{-2.06 \times 10^3}{\sqrt{g^*}} \left(\frac{m_4}{\text{eV}} \right) (U_{e4}^2 + 1.29 U_{\mu 4}^2) \right] \\ &\simeq 1 - \exp \left[-6.51 \times 10^2 \left(\frac{m_4}{\text{eV}} \right) (U_{e4}^2 + 1.29 U_{\mu 4}^2) \right]. \end{aligned} \quad (\text{A12})$$

A similar formula holds for the abundance of ν_r , upon replacement of index: $4 \rightarrow 5$. Note that the result in Eq. (A12) can be rewritten in terms of a single, effective, $\nu_e - \nu_s$ system, with mixing angle $\sin^2 2\theta_{\text{eff}} = 4(U_{e4}^2 + 1.29 U_{\mu 4}^2)$.

We find that our analytic solution, Eqn. (A12), gives results around 10% lower than our numeric solution at Points 1,2,3 in Table I. The main source of this discrepancy is g^* , which is kept fixed in the analytic solution, while its full temperature dependence is included in our numeric results. When g^* is kept fixed in both calculations, results match to within 5%.

-
- [1] R. Cowsik and J. McClelland, Phys.Rev.Lett. **29**, 669 (1972).
 - [2] G. Steigman, D. N. Schramm, and J. E. Gunn, Phys. Lett. **B66**, 202 (1977).
 - [3] L. M. Krauss and P. Romanelli, Astrophys. J. **358**, 47 (1990).
 - [4] P. J. Kernan and L. M. Krauss, Phys. Rev. Lett. **72**, 3309 (1994), astro-ph/9402010.
 - [5] G. Mangano *et al.*, Nucl. Phys. **B729**, 221 (2005), arXiv:hep-ph/0506164.
 - [6] L. M. Krauss, C. Lunardini, and C. Smith, (2010), arXiv:1009.4666 [hep-ph].
 - [7] S. Hannestad, I. Tamborra, and T. Tram, (2012), arXiv:1204.5861 [astro-ph.CO].
 - [8] S. Palomares-Ruiz, S. Pascoli, and T. Schwetz, JHEP **0509**, 048 (2005), arXiv:hep-ph/0505216 [hep-ph].
 - [9] E. Ma, G. Rajasekaran, and I. Stancu, Phys.Rev. **D61**, 071302 (2000), arXiv:hep-ph/9908489 [hep-ph].
 - [10] M. Cirelli, G. Marandella, A. Strumia, and F. Vissani, Nucl. Phys. **B708**, 215 (2005), arXiv:hep-ph/0403158.
 - [11] A. Melchiorri, O. Mena, S. Palomares-Ruiz, S. Pascoli, A. Slosar, *et al.*, JCAP **0901**, 036 (2009), arXiv:0810.5133 [hep-ph].
 - [12] C. Boehm, M. J. Dolan, and C. McCabe, (2012), arXiv:1207.0497 [astro-ph.CO].
 - [13] D. Hooper, F. S. Queiroz, and N. Y. Gnedin, Phys.Rev. **D85**, 063513 (2012), arXiv:1111.6599 [astro-ph.CO].
 - [14] Y. I. Izotov and T. X. Thuan, Astrophys. J. **710**, L67 (2010), arXiv:1001.4440 [astro-ph.CO].
 - [15] E. Aver, K. A. Olive, and E. D. Skillman, JCAP **1005**, 003 (2010), arXiv:1001.5218 [astro-ph.CO].
 - [16] E. Aver, K. A. Olive, and E. D. Skillman, JCAP **1204**, 004 (2012), arXiv:1112.3713 [astro-ph.CO].
 - [17] G. Mangano and P. D. Serpico, Phys.Lett. **B701**, 296 (2011), arXiv:1103.1261 [astro-ph.CO].
 - [18] K. M. Nollett and G. P. Holder, (2011), arXiv:1112.2683 [astro-ph.CO].
 - [19] J. Hamann, S. Hannestad, G. G. Raffelt, and Y. Y. Y. Wong, JCAP **1109**, 034 (2011), arXiv:1108.4136 [astro-ph.CO].
 - [20] Z. Hou, C. Reichardt, K. Story, B. Follin, R. Keisler, *et al.*, (2012), arXiv:1212.6267 [astro-ph.CO].
 - [21] G. Hinshaw, D. Larson, E. Komatsu, D. Spergel, C. Bennett, *et al.*, (2012), arXiv:1212.5226 [astro-ph.CO].
 - [22] T. Mueller, D. Lhuillier, M. Fallot, A. Letourneau, S. Cormon, *et al.*, Phys.Rev. **C83**, 054615 (2011), arXiv:1101.2663 [hep-ex].
 - [23] G. Mention, M. Fechner, T. Lasserre, T. Mueller, D. Lhuillier, *et al.*, Phys.Rev. **D83**, 073006 (2011), arXiv:1101.2755 [hep-ex].
 - [24] C. Giunti and M. Laveder, Phys.Rev. **C83**, 065504 (2011), arXiv:1006.3244 [hep-ph].
 - [25] F. Kaether, W. Hampel, G. Heusser, J. Kiko, and T. Kirsten, Phys.Lett. **B685**, 47 (2010), arXiv:1001.2731 [hep-ex].
 - [26] J. Abdurashitov *et al.* (SAGE Collaboration), Phys.Rev. **C80**, 015807 (2009), arXiv:0901.2200 [nucl-ex].
 - [27] A. Aguilar *et al.* (LSND), Phys. Rev. **D64**, 112007 (2001), arXiv:hep-ex/0104049.
 - [28] A. Aguilar-Arevalo *et al.* (MiniBooNE Collaboration), Phys.Rev.Lett. **102**, 101802 (2009), arXiv:0812.2243

- [29] [hep-ex].
- [30] A. Aguilar-Arevalo *et al.* (MiniBooNE Collaboration), Phys.Rev.Lett. **103**, 111801 (2009), arXiv:0904.1958 [hep-ex].
- [31] A. A. Aguilar-Arevalo *et al.* (The MiniBooNE), (2010), arXiv:1007.1150 [hep-ex].
- [32] A. Aguilar-Arevalo, B. Brown, L. Bugel, G. Cheng, E. Church, *et al.*, (2012), arXiv:1207.4809 [hep-ex].
- [33] M. Maltoni and T. Schwetz, Phys.Rev. **D76**, 093005 (2007), arXiv:0705.0107 [hep-ph].
- [34] J. Kopp, M. Maltoni, and T. Schwetz, Phys.Rev.Lett. **107**, 091801 (2011), arXiv:1103.4570 [hep-ph].
- [35] C. Giunti and M. Laveder, Phys.Rev. **D84**, 073008 (2011), arXiv:1107.1452 [hep-ph].
- [36] K. Abazajian, M. Acero, S. Agarwalla, A. Aguilar-Arevalo, C. Albright, *et al.*, (2012), arXiv:1204.5379 [hep-ph].
- [37] J. Conrad, C. Ignarra, G. Karagiorgi, M. Shaevitz, and J. Spitz, (2012), arXiv:1207.4765 [hep-ex].
- [38] M. Archidiacono, N. Fornengo, C. Giunti, and A. Melchiorri, (2012), arXiv:1207.6515 [astro-ph.CO].
- [39] K. Enqvist, K. Kainulainen, and M. J. Thomson, Nucl. Phys. **B373**, 498 (1992).
- [40] S. Riemer-Sorensen, D. Parkinson, T. Davis, and C. Blake, (2012), arXiv:1210.2131 [astro-ph.CO].
- [41] E. Giusarma, R. de Putter, and O. Mena, (2012), arXiv:1211.2154 [astro-ph.CO].
- [42] X. Wang, X.-L. Meng, T.-J. Zhang, H. Shan, Y. Gong, *et al.*, (2012), arXiv:1210.2136 [astro-ph.CO].
- [43] B. Benson, T. de Haan, J. Dudley, C. Reichardt, K. Aird, *et al.*, (2011), arXiv:1112.5435 [astro-ph.CO].
- [44] S. Joudaki, K. N. Abazajian, and M. Kaplinghat, (2012), arXiv:1208.4354 [astro-ph.CO].
- [45] For massive neutrinos that are not in a thermal distribution, the neutrino temperature T_ν is not a meaningful physical quantity. However, the equivalent temperature of a massless neutrino is used throughout this work, as it is still valid as a convenient measure of time. $T_\nu = \left(\frac{4}{11}\right)^{\frac{1}{3}} T_\gamma$, $T_\gamma = T_0(1+z)$, and the scale factor $a = \frac{1}{1+z}$.
- [46] S. Dodelson, A. Melchiorri, and A. Slosar, Phys.Rev.Lett. **97**, 041301 (2006), arXiv:astro-ph/0511500 [astro-ph].
- [47] As this manuscript was being prepared, Ref. [53] performed a similar calculation of the effect of neutrino mass on N_{eff} . Whilst our expression for the neutrino phase-space distribution, Eqn. (20), agrees with their Eqn. (8), we reach a different conclusion regarding the effect on N_{eff} , which measures the energy density in *relativistic* neutrinos, rather than the total neutrino energy density.
- [48] R. Foot and R. R. Volkas, Phys. Rev. Lett. **75**, 4350 (1995).
- [49] P. Di Bari, P. Lipari, and M. Lusignoli, Int.J.Mod.Phys. **A15**, 2289 (2000), arXiv:hep-ph/9907548 [hep-ph].
- [50] K. Abazajian, G. M. Fuller, and M. Patel, Phys. Rev. **D64**, 023501 (2001), arXiv:astro-ph/0101524.
- [51] R. Foot and R. R. Volkas, Phys. Rev. **D55**, 5147 (1997), arXiv:hep-ph/9610229.
- [52] S. Dodelson and L. M. Widrow, Phys. Rev. Lett. **72**, 17 (1994), arXiv:hep-ph/9303287.
- [53] The hierarchy between the oscillation length and the mean free path is weak for $T \gtrsim 30$ MeV, and so one may doubt the accuracy of our equation. In Ref. [50] a more sophisticated equation is given, that does not rely on the hierarchy of lengths. We have checked numerically that this equation and Eqn. (A6) give very similar results. Therefore, we consider Eqn. (A6) for the sake of simplicity.
- [54] J. Birrell, C.-T. Yang, P. Chen, and J. Rafelski, (2012), arXiv:1212.6943 [astro-ph.CO].